

Correlation-Aware User Selection for Cooperative Spectrum Sensing in Cognitive Radio Ad Hoc Networks

Angela Sara Cacciapuoti, *Member, IEEE*, Ian F. Akyildiz, *Fellow, IEEE*, and Luigi Paura, *Member, IEEE*

Abstract—This paper develops a solution for the problem of uncorrelated user selection in mobile cognitive radio ad hoc networks, with the objective to increase the performance of cooperative spectrum sensing. For this, a fully distributed user selection algorithm is developed by adaptively selecting uncorrelated cognitive radio users, which is able to account for dynamic changes in the network topology and in the channel conditions. Since the proposed user selection is based on the evaluation of the correlation experienced by the cognitive radio users, it is mandatory to have a parameter able to measure the correlation among them. For this, a spatial correlation coefficient is proposed to express the correlation characteristics of mobile cognitive radio users in different environments. Performance evaluation is conducted through simulations, and the results reveal the benefits of adopting the proposed correlation-aware user selection for cooperative spectrum sensing.

Index Terms—User Selection, Correlation Model, Cooperative Spectrum Sensing, Cognitive Radio.

I. INTRODUCTION

SPECTRUM Sensing is a key functionality in Cognitive Radio (CR) Networks [1]. Through spectrum sensing, unlicensed users (CR users) can recognize and exploit portions of the radio spectrum whenever they are vacated by licensed users (Primary Users (PUs)). The spectrum sensing functionality can be implemented in either a non-cooperative or a cooperative fashion. In the former, each CR user autonomously recognizes the available portions of the spectrum; in the latter, the CR users exchange sensing information to take decisions on the PU presence [2]. Cooperative approaches have been proposed to counteract the wireless channel impairments, such as multipath and/or shadow fading, by exploiting the spatial diversity among the CR users [3]–[6]. However, the cooperation among many CR users may also introduce overhead that limits or even compromises the achievable cooperative gain [2].

Spatial correlation affects the performance of cooperative sensing. Spatially close CR users are likely to be affected by the same environmental conditions, and they can suffer

Manuscript received 15 February 2011; revised 20 June 2011. This work was supported by the Italian National Program Industria 2015 under the project “Global & Reliable End to End e-Commerce & On Line Service Platform (GRECO)” and by the U.S. National Science Foundation under Award ECCS-0900930.

A. S. Cacciapuoti and I. F. Akyildiz are with Broadband Wireless Networking Laboratory, School of Electrical and Computer Engineering, Georgia Institute of Technology, Atlanta, USA (e-mail: ian@ece.gatech.edu).

L. Paura is with the Dept. of Biomedical, Electronics and Telecommunications Engineering University of Naples Federico II, Naples, Italy (e-mail: paura@unina.it).

Digital Object Identifier 10.1109/JSAC.2012.120208.

from common biases in the spectrum sensing. CR users that are farther apart can benefit from their different geographical locations, and obtain a more reliable and unbiased recognition of the available spectrum portions. In fact, in [3], [7] it has been proven that having a small number of farther located CR users may be more effective than having a large number of closely located CR users. Hence, the selection of uncorrelated CR users is key to improve the robustness of the sensing results. Furthermore, the use of a lower number of CR users helps reducing the overhead inherent to the cooperative approaches.

New challenges arise in the selection of cooperating CR users when the users are mobile. Mobility changes the mutual distances of the CR users and, consequently, it varies dynamically their correlation. The selection of cooperating CR users should be adaptive with respect to these correlation changes.

In this paper, we develop a correlation-aware user selection to address the dynamic changes in the spatial correlation experienced by mobile CR users, with the objective to increase the performance of cooperative spectrum sensing.

For this, we design a fully distributed selection algorithm which adaptively selects uncorrelated CR users in CR Ad Hoc Networks (CRAHNs) [8]. The proposed algorithm accounts for dynamic changes in the network topology and in the channel conditions. Since the proposed selection strategy is based on the evaluation of the correlation experienced by the CR users, it is mandatory to have a parameter which measures the correlation among them. For this, we propose a spatial correlation coefficient, which captures the correlation characteristics of mobile CR users. Specifically, the contributions made in this paper are: *i*) the development of a correlation model to accurately derive the spatial correlation coefficient between mobile CR users; *ii*) the design of a fully distributed user selection algorithm able to adaptively select uncorrelated CR users through the spatial correlation coefficient.

The rest of the paper is organized as follows. In Section II, we formulate the problem. In Section III, we derive the spatial correlation coefficient. In Section IV, we design the user selection strategy. We evaluate the spatial correlation coefficient and the user selection algorithm in Section V. Finally, in Section VI, we conclude the paper.

II. PROBLEM STATEMENT

In cooperative spectrum sensing, a CR user cooperates with other CR users to perform opportunistic spectrum access. In correlated scenarios, a user selection is required, since the correlation affects the performance of cooperative sensing.

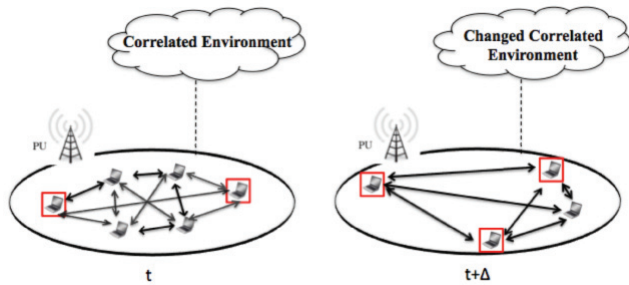


Fig. 1. The proposed strategy selects the less correlated CR users according to the changes in the network topology and in the channel conditions.

A. Challenges

The design of a user selection strategy suitable for mobile CRAHNs arises several challenges:

- the selection should be *fully distributed*, i.e., it should avoid the need of a central entity that handles the mechanism, since CRAHNs lack centralized support;
- the selection should be *adaptive*, i.e., it should be able to track the dynamical changes of the correlation experienced by the CR users due to the changes in the network topology and in the channel conditions;
- the selection should be *location-unaware*, i.e., it should not require the knowledge of the CR user positions.

The property of location unawareness is attractive when:

- dedicated positioning systems (e.g. GPS) cannot be used by the CR users for concerns due to *i)* cost, since they require additional hardware; *ii)* functionality, since they cannot be used yet for indoor applications;
- the distribution/estimation of the position information in the network cannot be supported since it introduces excessive communication overhead.

B. Proposed Selection Strategy

We consider a scenario in which M neighboring CR users can cooperate through a common control channel (CCC) [2]. The goal is to select a set of CR users out of M that experience the lowest correlation. For this, we propose a selection strategy based on the evaluation of the correlation experienced by the CR users through a general parameter, i.e., the *spatial correlation coefficient*, which measures the correlation among them. The proposed algorithm exhibits several attractive features:

- 1) The algorithm is fully distributed. As shown in Fig. 1, the CR users cooperate for selecting the uncorrelated CR users, denoted in the figure with the red squares, without the need of a central entity deputed to the selection.
- 2) The algorithm is iterative and adaptive to the network topology and the channel conditions. The adaptive feature is shown in Fig. 1, where some CR users are considered in two different times, t and $t + \Delta$. The correlation experienced by the CR users at time t and at time $t + \Delta$ can be different, due to either CR mobility or changes in the channel conditions. Through the evaluation of the correlation coefficients and the iterative implementation of the algorithm, our user selection strategy is able

to detect these dynamics in the spatial correlation by selecting different CR users, as shown in Fig. 1.

- 3) The algorithm is location-unaware, since all the information required by the algorithm are obtained by measuring the correlation coefficients between CR users.

C. Related Work

User Selection: In [9], three centralized location-aware selection schemes are proposed for cooperative sensing to address the shadow correlation problem in a cellular system. These algorithms are performed at the fusion center, by exploiting different degrees of knowledge about the CR user positions. The authors show that their algorithms perform better than the random selection. The centralized selection may be affected by high overhead [2]. Grouping the cooperating CR users into clusters can be an effective way to alleviate this problem. In [10], different clustering methods are proposed by using the availability of location information. The authors show that more reliable sensing can be achieved when the position of PUs is known. Unlike all the aforementioned works, the proposed selection strategy is location-unaware and it does not require the presence of a central entity.

Spatial Correlation Model: In this paper, we consider both the shadow and the multipath fading. Regarding the shadow fading, in [11] Gudmundson proposes an effective correlation model, proving that the shadowing is ordinarily correlated. In Section III, we use this model to define the correlation coefficient for shadow fading. Regarding the multipath fading, a great bulk of research has been devoted to develop statistical autocorrelation models for time-variant multipath channels, starting from the seminal work in [12]. Recently, the attention is focused on the multi-element antenna systems, for which [13] derives an interesting space-time correlation model. Nevertheless, such a model cannot be directly applied to describe the correlation among CR users, since it is based on the assumption that in an antenna array the distance between the elements is fixed. Hence, a more general model that accounts for the CR mobility is necessary to quantify the correlation in multipath environment. In Section III, we address this issue.

III. SPATIAL CORRELATION COEFFICIENT

In the following, we derive the spatial correlation coefficient for both the shadow and the multipath fading environments.

A. Signal Model

The base-band received sensing signal $x_i(t)$ at the i -th CR user during the sensing interval T_s can be written as [2]:

$$x_i(t) = \begin{cases} v_i(t) & \mathcal{H}_0 \\ g_i(t) s(t) + v_i(t) & \mathcal{H}_1 \end{cases} \quad t \in [0, T_s] \quad (1)$$

where $s(t)$ is the PU signal, which we consider to be deterministic and unknown [14], [15]. $g_i(t)$ is the time-variant channel gain that models either a shadow or a frequency non-selective multipath fading channel. $v_i(t) \sim \mathcal{N}(0, \sigma_n^2)$ is the additive white Gaussian noise. \mathcal{H}_0 and \mathcal{H}_1 denote the hypotheses of “no PU signal” and “PU signal transmitted”, respectively.

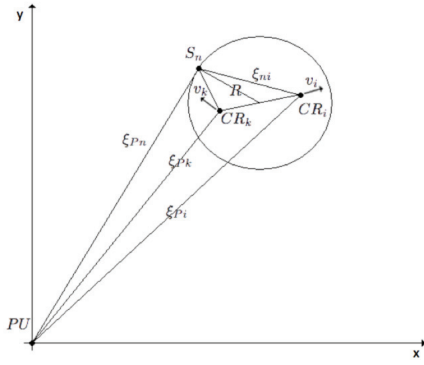


Fig. 2. Geometrical picture with local scatterer around mobile CR users

B. Spatial Correlation Coefficient

Definition 1: The spatial correlation coefficient at time t of two sensing signals is the ratio between their covariance at time t and the product of their standard deviations at time t :

$$c_{ik}(t) \triangleq \frac{\text{COV}[x_i(t), x_k(t)]}{\sigma_{x_i}(t) \sigma_{x_k}(t)} \quad (2)$$

By substituting (1) in (2), $c_{ik}(t)$ can be rewritten as:

$$c_{ik}(t) = \begin{cases} 0 & \mathcal{H}_0 \\ \frac{\rho_{ik}(t) \sigma_{g_i}(t) \sigma_{g_k}(t) E_s(t) + \sigma_n^2 \delta(i-k)}{\sigma_{x_i}(t) \sigma_{x_k}(t)} & \mathcal{H}_1 \end{cases} \quad (3)$$

where, $E_s(t) \triangleq |s(t)|^2$ is the PU energy at time t , $\delta(m)$ is the Kronecker delta, and $\rho_{ik}(t)$ is the spatial correlation coefficient of the sensing channels $g_i(t)$ and $g_k(t)$, which is defined as:

$$\rho_{ik}(t) \triangleq \frac{\text{COV}[g_i(t), g_k(t)]}{\sigma_{g_i}(t) \sigma_{g_k}(t)} \quad (4)$$

From (3), it results that if $|\rho_{ik}(t)| \neq 0$, also the sensing signals are correlated $|c_{ik}(t)| \neq 0$. In the following, we investigate the correlation effects by exploiting $\rho_{ik}(t)$.

C. Spatial Correlation Coefficient for Shadow Fading

For shadow fading, (4) can be expressed as [11]:

$$\rho_{ik}(t) = e^{-d_{ik}(t)/D} \quad (5)$$

where $d_{ik}(t)$ is the distance between the i -th and the k -th CR user, and D is the decorrelation distance, whose value depends on the environment [16]. By substituting (5) in (3), $c_{ik}(t)$ for correlated shadow fading is obtained:

$$c_{ik}(t) = \begin{cases} 0 & \mathcal{H}_0 \\ \frac{e^{-d_{ik}(t)/D} \sigma_{g_i}(t) \sigma_{g_k}(t) E_s(t) + \sigma_n^2 \delta(i-k)}{\sigma_{x_i}(t) \sigma_{x_k}(t)} & \mathcal{H}_1 \end{cases} \quad (6)$$

D. Spatial Correlation Coefficient for Multipath Fading

Definition 2: The space-time cross-correlation $R_{ik}(t, \tau)$ between two sensing channels $g_i(t)$ and $g_k(t)$ is defined as:

$$R_{ik}(t, \tau) \triangleq E[g_i(t) g_k^*(t - \tau)] \quad (7)$$

where $(\cdot)^*$ denotes the complex conjugate operator. By using (7) and the relation between the covariance and the correlation

of random variables (r.v.s.) [17], (4) can be written as function of the space-time cross-correlation at $\tau = 0$:

$$\rho_{ik}(t) = \frac{R_{ik}(t, 0) - E[g_i(t)] E^*[g_k(t)]}{\sigma_{g_i}(t) \sigma_{g_k}(t)} \quad (8)$$

To fully determine (8), we first derive $R_{ik}(t, \tau)$. For this, $g_i(t)$ is divided into two contributions [13], i.e., the deterministic contribution $g_{i,\text{LOS}}(t)$ due to the Line of Sight (LOS) path, and the random contribution $g_{i,\text{DIF}}(t)$ (referred to as diffuse component) that includes the paths generated by the ring of scatterers enclosing the CR user:

$$g_i(t) = g_{i,\text{DIF}}(t) + g_{i,\text{LOS}}(t) \quad (9)$$

with

$$g_{i,\text{LOS}}(t) = |g_{i,\text{LOS}}(t)| e^{-j\left(\frac{2\pi}{\lambda} \xi_{P_i} - 2\pi f_{D_i} t \cos(\phi_{P_i} - \gamma_i)\right)} \quad (10)$$

$$g_{i,\text{DIF}}(t) = \sum_{n=1}^N \alpha_n e^{j\left(\psi_n - 2\pi \left[\frac{\xi_{P_n} + \xi_{ni}(\phi_{ni})}{\lambda} - f_{D_i} t \cos(\phi_{ni} - \gamma_i)\right]\right)} \quad (11)$$

In (10) and (11), N is the number of independent scatterers around the CR users, α_n is the amplitude of the wave scattered by the n -th scatterer S_n , ψ_n denotes the phase shift introduced by S_n , and ξ_{P_n} is the distance between the PU and S_n . ξ_{ni} is the distance between S_n and the i -th CR user, and it is a function of the Angle Of Arrival (AOA) ϕ_{ni} between S_n and the i -th CR user. λ is the wavelength of the PU transmission, γ_i identifies the direction of the i -th CR user movement characterized by a velocity v_i . $f_{D_i} = \frac{v_i}{\lambda}$ is the maximum Doppler frequency, ϕ_{P_i} and ξ_{P_i} indicate the AOA and the length of the LOS path, respectively (see Fig. 2). $\{\alpha_n\}$ is a set of independent positive r.v.s. with finite variance, independent of the set $\{\psi_n\}$, which contains i.i.d r.v.s., uniformly distributed in $[0, 2\pi)$, [12], [13]. Since $g_{i,\text{DIF}}(t)$ and $g_{k,\text{DIF}}(t)$ are zero-mean random processes, by substituting (9) in (7), $R_{ik}(t, \tau)$ is expressed as function of the space-time cross-correlations of the diffuse $R_{ik}^{\text{DIF}}(t, \tau) \triangleq E[g_{i,\text{DIF}}(t) g_{k,\text{DIF}}^*(t - \tau)]$ and of the LOS components $R_{ik}^{\text{LOS}}(t, \tau) \triangleq g_{i,\text{LOS}}(t) g_{k,\text{LOS}}^*(t - \tau)$:

$$R_{ik}(t, \tau) = R_{ik}^{\text{DIF}}(t, \tau) + R_{ik}^{\text{LOS}}(t, \tau) \quad (12)$$

To derive $R_{ik}(t, \tau)$, we adopt a non-isotropic scattering model, since the AOA distribution is more likely to be nonuniform [18]. For this, we utilize the von Mises distribution that fits very well with experimental data [13], [19], whose Probability Density Function (PDF) is equal to $f(\phi) = e^{\zeta \cos(\phi - \mu)} / (2\pi I_0(\zeta))$, $|\phi| < \pi$, where $I_0(\cdot)$ is the zero-order modified Bessel function, $\mu \in [-\pi, \pi)$ is the AOA mean, and $\zeta \geq 0$ controls the width of the AOA. $\zeta = 0$ corresponds to isotropic scattering, i.e., $f(\phi) = \frac{1}{2\pi}$, $|\phi| < \pi$.

Proposition 1: The space-time cross-correlation of the diffuse components $R_{ik}^{\text{DIF}}(t, \tau)$ is given by:

$$R_{ik}^{\text{DIF}}(t, \tau) = \frac{P_r^{\text{DIF}}}{I_0(\zeta)} I_0 \left\{ \left[\zeta^2 - b_{ik}^2 - a_i^2(t) - a_k^2(t - \tau) + 2a_i(t)a_k(t - \tau) \cos(\gamma_i - \gamma_k) - 2j\zeta [b_{ik} \cos(\mu - \theta_{ik}) + -a_i(t) \cos(\mu - \gamma_i) + a_k(t - \tau) \cos(\mu - \gamma_k)] + 2b_{ik} [a_i(t) \cos(\mu - \gamma_i) - a_k(t - \tau) \cos(\mu - \gamma_k)] \right]^{1/2} \right\} \quad (13)$$

Proof: See Appendix A. ■

In (13), P_r^{DIF} is the diffuse power, $b_{ik} \triangleq \frac{2\pi}{\lambda} d_{ik}$ (d_{ik} is the initial CR distance). $\{a_l(t) \triangleq 2\pi f_{D_l} t\}_{l=i,k}$ accounts for the CR mobility and hence for the changes in CR mutual distance.

Proposition 2: The space-time cross-correlation of the LOS components $R_{ik}^{\text{LOS}}(t, \tau)$ is given by:

$$R_{ik}^{\text{LOS}}(t, \tau) = |g_{i,\text{LOS}}(t)| |g_{k,\text{LOS}}(t - \tau)| e^{j b_{ik} \cos(\theta_{ik})} e^{-j[a_i(t) \cos(\gamma_i) - a_k(t - \tau) \cos(\gamma_k)]} \quad (14)$$

Proof: See Appendix B. ■

By combining (13) and (14) in (12), the closed form expression of $R_{ik}(t, \tau)$ is obtained in the general case of non-isotropic scattering. Stemming from this analysis, we evaluate the spatial correlation coefficient $\rho_{ik}(t)$ (8) for multipath channels. Since $E[g_i(t)] E^*[g_k(t)] = R_{ik}^{\text{LOS}}(t, 0)$, (8) becomes:

$$\rho_{ik}(t) = \frac{R_{ik}(t, 0) - R_{ik}^{\text{LOS}}(t, 0)}{\sigma_{g_i}(t) \sigma_{g_k}(t)} = \frac{R_{ik}^{\text{DIF}}(t, 0)}{\sigma_{g_i}(t) \sigma_{g_k}(t)} \quad (15)$$

By using (13) in (15), $\rho_{ik}(t)$ is given by:

$$\rho_{ik}(t) = \frac{1}{I_0(\zeta)} I_0 \left\{ \left[\zeta^2 - b_{ik}^2 - a_i^2(t) - a_k^2(t) + 2a_i(t)a_k(t) \cos(\gamma_i - \gamma_k) - 2j\zeta [b_{ik} \cos(\mu - \theta_{ik}) - a_i(t) \cos(\mu - \gamma_i) + a_k(t) \cos(\mu - \gamma_k)] + 2b_{ik}[a_i(t) \cos(\mu - \gamma_i) - a_k(t) \cos(\mu - \gamma_k)] \right]^{1/2} \right\} \quad (16)$$

By substituting (15) in (3), $c_{ik}(t)$ is obtained:

$$c_{ik}(t) = \begin{cases} 0 & \mathcal{H}_0 \\ \frac{R_{ik}^{\text{DIF}}(t, 0) E_s(t) + \sigma_n^2 \delta(i-k)}{\sigma_{x_i}(t) \sigma_{x_k}(t)} & \mathcal{H}_1 \end{cases} \quad (17)$$

Remark 1: $R_{ik}(t, \tau)$ degenerates into the Clarke's temporal autocorrelation [12], if $\zeta = 0$, no LOS and $i \equiv k$, and into the result derived in [13], [19] if $\zeta \neq 0$, no LOS and $i \equiv k$.

Remark 2: In [19], the authors show that for non-isotropic scattering the autocorrelation can be larger than the Clarke's autocorrelation. Hence, the coherence time $(\Delta t)_c$ for isotropic scattering is generally smaller than the coherence time for non-isotropic scattering, $(\Delta t)_c^{\text{isotropic}} \leq (\Delta t)_c^{\text{non-isotropic}}$, i.e., the time-variability of a sensing channel modeled with the Clarke's model is larger than that associated with the non-isotropic case. For this, to assure that a sensing channel is stationary during the sensing process, T_s must be set according to the condition $T_s < (\Delta t)_c^{\text{isotropic}} \simeq 0.5/f_D$ [12]. E.g., if the PU transmission frequency is $f_c = 1$ GHz, and if $v = 28$ m/s (vehicular velocity), $T_s < (\Delta t)_c \simeq 5$ ms (for pedestrian velocities $(\Delta t)_c$ increases). More in general, for pedestrian and vehicular patterns, and for the commonly used f_c , the stationary sensing channel assumption appears to be reasonable.

IV. CORRELATION-AWARE USER SELECTION

Here, first we present the correlation-aware selection strategy, then we describe the distributed algorithm in detail.

A. Correlation-Aware Selection Strategy

To find in a distributed way a set of CR users out of M that experience the lowest correlation, without requiring

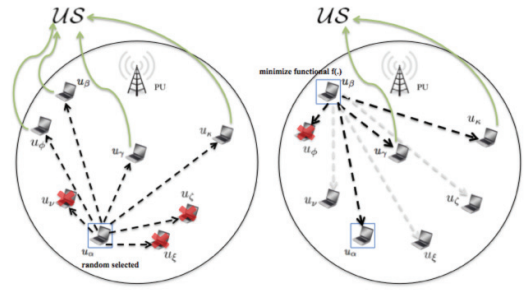


Fig. 3. Correlation-Aware Selection Algorithm

the knowledge about their mutual distances, we propose a selection strategy based on the estimation of the correlation coefficients (2) of the sensing signals $\{x_l(t)\}$ through a temporal mean:

$$\hat{c}_{ik}(t) = \frac{\langle (x_i(t) - \hat{\mu}_i(t))(x_k(t) - \hat{\mu}_k(t))^* \rangle}{\langle |x_i(t) - \hat{\mu}_i(t)|^2 \rangle \langle |x_k(t) - \hat{\mu}_k(t)|^2 \rangle} \quad (18)$$

where $\langle \cdot \rangle$ denotes the temporal mean operator on T_s , and $\hat{\mu}_i(t)$ and $\hat{\mu}_k(t)$ indicate the temporal means of $x_i(t)$ and $x_k(t)$, respectively. We assume that during the sensing process time I_s (that includes T_s , the time to select the cooperative CR users and to make the final decision) the correlations among the mobile CR users do not change significantly. This is reasonable for vehicular or pedestrian mobility, since in the short sensing process time, generally considered in practice (e.g. $I_s < 1$ sec), the CR users cannot change significantly their mutual distances. In Sec. IV-B, we detail how to obtain efficiently the sensing signal $\{x_k(t)\}_{k \neq i}$ to perform the estimations $\{\hat{c}_{ik}(t)\}$.

B. Correlation-Aware Selection Algorithm

The proposed algorithm is iterative, and each iteration consists of two steps: *pruning* and *election*. The former step discards the correlated CR users, i.e. the CR users that estimate a correlation coefficient (18) above a certain threshold ϵ_d . The latter step singles out among the remaining users the CR user with the lowest value of the correlation-based functional $\mathcal{F}(\cdot)$, as described in the following.

Specifically, the algorithm is randomly initialized, i.e. a CR user, referred to as u_α , is randomly selected among the M neighbors to broadcast its sensing information on the CCC. The remaining CR users listen to this transmission to estimate their correlation coefficients $\{\hat{c}_{\alpha k}(t)\}_{k=1, k \neq \alpha}^M$. Then, they compare the estimated coefficients with the threshold ϵ_d . If the estimated coefficient is above ϵ_d , the CR user considers itself correlated with u_α , and it does not take part in the subsequent iterations of the algorithm. Otherwise, the CR user considers itself uncorrelated. We denote the set of uncorrelated CR users with \mathcal{US} . The CR user belonging to \mathcal{US} that minimizes the functional $\mathcal{F}(\cdot)$, i.e., the CR user having the smallest estimated correlation coefficient with the CR user u_α , is *elected* to transmit its sensing information. We refer to this CR user as u_β . At this point, the above described procedure is repeated: the remaining CR users in \mathcal{US} estimate their correlation coefficients $\{\hat{c}_{\beta i}(t)\}_{i \in \mathcal{US} \text{ with } i \neq \beta}$, and compare them with ϵ_d . If the estimated coefficient is

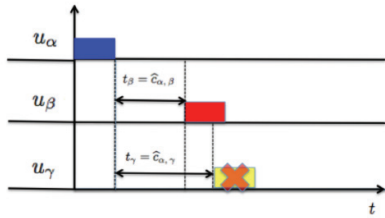


Fig. 4. Example of distributed implementation of the proposed algorithm

above the threshold ϵ_d , the CR user considers itself correlated with the u_β , and it does not take part in the subsequent iterations of the algorithm. Otherwise, the CR user considers itself uncorrelated with the CR user u_β . Among the CR users uncorrelated with u_β , the CR user that minimizes $\mathcal{F}(\cdot)$, i.e., the CR user with smallest estimated correlation coefficient with both u_β and u_α , is selected to send its sensing information to the remaining CR users. The above described process is depicted in Fig. 3. The algorithm continues iteratively until the convergence is reached, i.e., until the set \mathcal{US} becomes empty, and it provides as output the set \mathcal{S} of the selected CR users. These CR users in \mathcal{S} participate in the cooperative spectrum sensing. We summarize our algorithm in Algorithm 1, where we indicate with \mathcal{N} the set of neighbors.

Remark 1: Since the cardinality of the set \mathcal{S} is not fixed a-priori but it is determined by the algorithm itself, the proposed selection is able to adapt the number of selected CR users to different network topologies and channel conditions.

Remark 2: During the selection process, the CR users in \mathcal{S} collect the sensing information from each other. Hence, at the end of the selection, they are able to take the final decision on the presence of the PU, without the need of a further information sharing. This allows to save communication resources.

Remark 3: The proposed algorithm is fully distributed, since it does not need a central entity that handles the selection. In the following, we describe a possible way to implement our algorithm in a distributed manner. This implementation does not use explicit coordination communications among the CR users, thus limiting the communication overhead.

When the random selected CR user u_α transmits its sensing information, the remaining CR users are able to estimate their correlation coefficients, as described above. To select the CR user in \mathcal{US} with the smallest correlation coefficient, we can consider a timer mechanism based on the estimated coefficients. E.g., with reference to Fig. 4, we suppose that there are two CR users in the set \mathcal{US} , u_β and u_γ . Each of them sets a timer according to its estimated coefficient, so that the CR user with the lowest correlation coefficient sets the lowest timer. When the shorter timer expires, the corresponding CR user is allowed to transmit its sensing information, thus informing the neighbors that a CR user with a smaller correlation exists in the network. In the example depicted in Fig. 4, since u_β measures a correlation coefficient smaller than the coefficient of u_γ , the timer of u_β is shorter than the timer of u_γ , and hence, u_β transmits first, thus resulting in the selected CR user. The same mechanism can be applied for the subsequent iterations of the algorithm as well

Algorithm 1 Correlation-Aware Selection Algorithm

```

1:  $\mathcal{S} = \emptyset, \mathcal{US} = \emptyset$ 
2: // initialization: randomly selected  $u_\alpha$ 
3:  $\mathcal{S} \leftarrow \{u_\alpha\}$ 
4:  $\mathcal{US} \leftarrow \mathcal{N} - \{u_\alpha\}$ 
5:  $\text{best} \leftarrow u_\alpha$ 
6: while  $\mathcal{US} \neq \emptyset$  do
7:   // Pruning Step: the correlated CR users are removed from  $\mathcal{US}$ 
8:   for  $v \in \mathcal{US}$  do
9:     if  $\text{Correlation}(\text{best}, v) > \epsilon_d$  then
10:        $\mathcal{US} \leftarrow \mathcal{US} - \{v\}$ 
11:     end if
12:   end for
13:   // Election Step: Among the uncorrelated CR users the one that minimizes the
   functional  $\mathcal{F}(\cdot)$  is selected
14:   find  $u_\nu \in \mathcal{US}: \mathcal{F}(u_\nu, \mathcal{S}) = \min_{v \in \mathcal{US}} \mathcal{F}(v, \mathcal{S})$ 
15:    $\mathcal{S} \leftarrow u_\nu$ 
16:    $\mathcal{US} \leftarrow \mathcal{US} - \{u_\nu\}$ 
17:    $\text{best} \leftarrow u_\nu$ 
18: end while

```

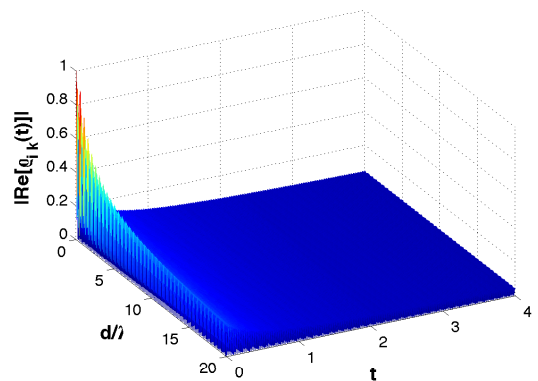


Fig. 5. $|\text{Re}[\rho_{ik}(t)]$ vs (d, t)

as for the random selection of the first CR user during the algorithm initialization. However, since the CR users cannot estimate the correlation during the initialization process, each of them sets the timer by randomly choosing a value in an interval $[0, T_{max}]$, where T_{max} is set according to the number/density of neighbors determined during the neighbor discovering process.

V. PERFORMANCE EVALUATION

In Sec. V-A, the proposed $\rho_{ik}(t)$ for multipath channels is analyzed. In Secs. V-B and V-C, we evaluate the performance of the proposed selection strategy for shadow and multipath fading.

A. Spatial Correlation Coefficient for Multipath Channels

The values of the decorrelation distance D for shadow fading range approximately from 30 to 100 m [11]. This information is not available for multipath fading. Therefore, we analyze the proposed $\rho_{ik}(t)$ (16) to quantify the amount of correlation experienced by two mobile CR users as a function of their distance. We assume without loss of generality that one CR user is static and the other moves.

In Fig. 5 we show the absolute value of the real part of $\rho_{ik}(t)$ versus the time and the mutual distance of the CR users normalized to λ , for $v = 28$ m/s (vehicular mobility), $\zeta = 5$, $\mu = \pi$ and $f_c = 900$ MHz. The results show

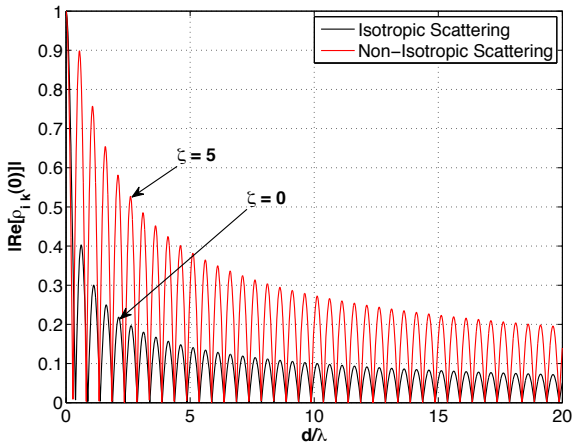
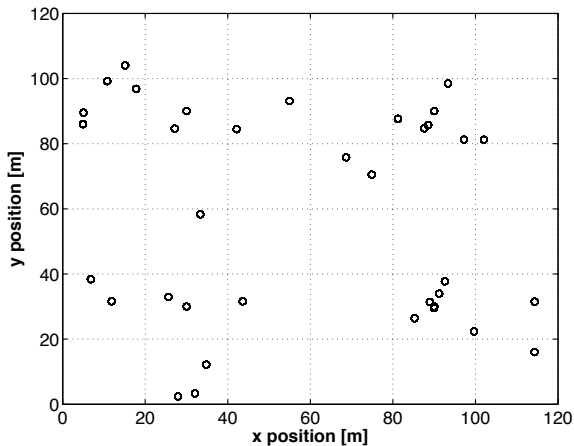
Fig. 6. $|\text{Re}[\rho_{ik}(0)]$ vs d 

Fig. 7. Top. 1 for Shadowing

that the correlation strongly depends on the distance, while it decays quickly with t . In Fig. 6 we show the section of Fig. 5 for $t = 0$. We note that at a distance of $20\lambda \simeq 7$ m, $|\text{Re}[\rho_{ik}(0)]| \simeq 0.2$. In Fig. 6, we report also the case of isotropic scattering, i.e., $\zeta = 0$, in which $|\text{Re}[\rho_{ik}(0)]| \simeq 0.2$ when $d \simeq 1$ m. Hence, in presence of isotropic scattering the correlation experienced by the CR users is smaller than the correlation experienced in presence of non-isotropic scattering. However, the AOA distribution is more likely to be nonuniform, specially in urban and suburban areas [18]. Similar considerations hold for pedestrian velocity and we do not report them for brevity. Our analysis, although not exhaustive, underlines that mobile CR users can experience correlated multipath fading. The distances at which the CR users experience significant correlation are in the order of 10 m in presence of non-isotropic scattering. Hence, the common assumption of uncorrelated CR users in multipath environments does not hold in all the possible scenarios.

B. Performance Analysis with Correlated Shadow Fading

Two topologies, Top. 1 and Top. 2 shown in Fig. 7 and Fig. 8, are considered. In both the topologies the number of CR users is $M = 36$, and the grid size is 120 x 120 m. $\{g_i\}_{i=1}^M$ are randomly-generated according to a log-normal distribution

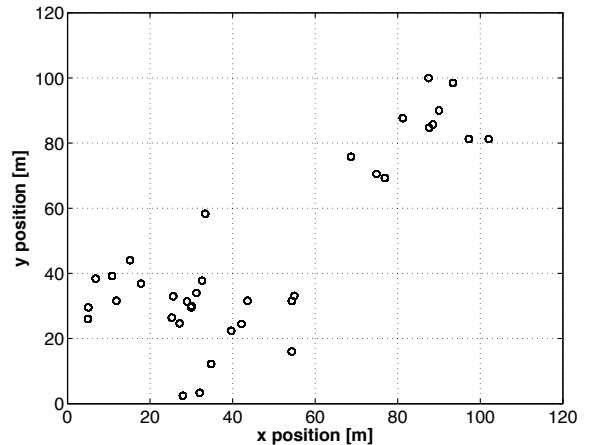
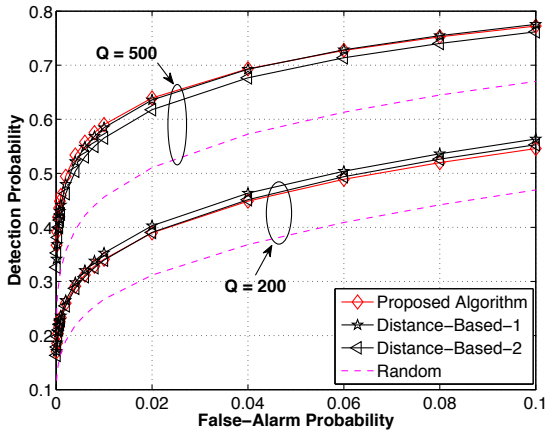
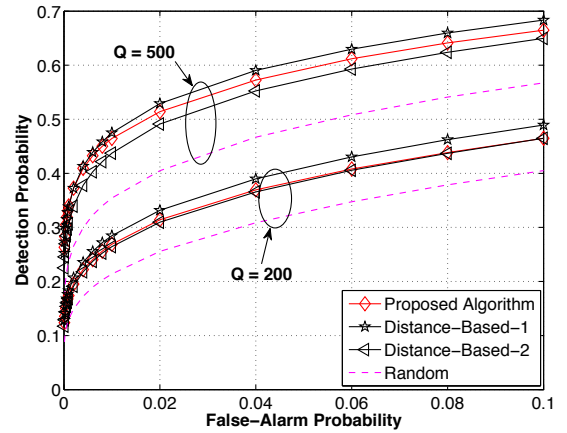


Fig. 8. Top. 2 for Shadowing

with zero-mean. To model the spatial correlation, we adopt the Gudmundson's model (5) for $D = 30$ m. The performances of the proposed selection are compared with the performances of two selection strategies: a distance-based and a random selection. For the distance-based we provide two implementations: *i*) Distance-Based-1, in which the algorithm is initialized by choosing the two furthest CR users and then it iteratively selects the CR user that has the largest distances from the previous selected CR users; *ii*) Distance-Based-2, in which the algorithm is initialized with the same CR user randomly selected by the proposed algorithm and then, it continues as described for the first implementation. Since the distance-based algorithms are iterative, they adaptively select the number of selected CR users. Regarding the random algorithm, we set the value of the number of selected CR users equal to that iteratively discovered by the proposed algorithm. The results are obtained through 10^5 independent Monte Carlo runs, by assuming that the arbitrary CR user in \mathcal{S} adopts an energy detector to combine the sensing information. In each run the noise samples are randomly and independently generated according to a zero-mean normal distribution. The average SNR within the considered area is set to $\overline{SNR} = -12$ dB. To overcome the whitening effect introduced on the sensing signals by the noise in such a low SNR scenario, we assume the presence of an ideal denoising processing on $\{x_i(t)\}$ before the correlation estimations. The transmitted PU signal has unitary power. To assess the impact of the sensing length on the performance of the algorithms, we consider two values for the number Q of samples [20] available in T_s , i.e. $Q = 500$ and $Q = 200$.

1) *Scenario A*: We evaluate the performance of the considered algorithms for the dB-spread $\sigma_{dB} = 8$ dB. Fig. 9 shows the Detection Probability P_d versus the False-Alarm Probability P_f for Top. 1 when $Q = 500$. P_f ranges from 10^{-4} to 10^{-1} . We set $\epsilon_d = e^{-1}$ to allow a fair comparison with the distance-based algorithms. In fact, these algorithms select the CR users that have mutual distances greater than D , i.e., they select the CR users that experience correlation coefficients (5) smaller than $\rho_{ik} = e^{-D/D} = e^{-1}$. We note that the proposed algorithm outperforms significantly the random selection, and it performs comparable with the two

Fig. 9. P_d vs P_f , Top. 1Fig. 10. P_d vs P_f , Top. 2TABLE I
AVERAGE ITERATION NUMBER

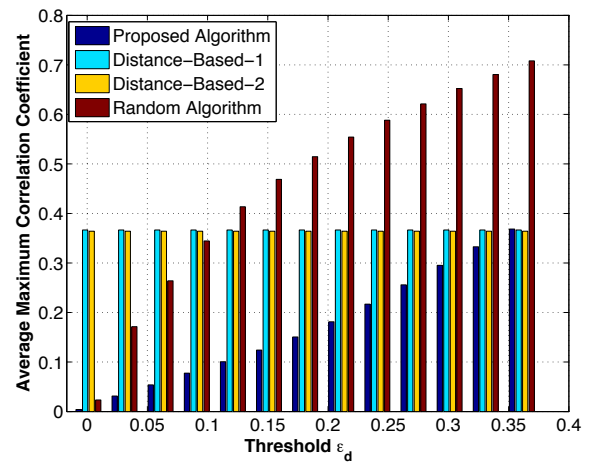
Topology	Correlation Aware	Distance Based-1	Distance Based-2
Top. 1 Shadowing	5.9664	9	8.5160
Top. 2 Shadowing	3.8483	6	5.1830
Top. 1 Multipath	5.7856	7	6.4847
Top. 2 Multipath	8.2606	8	7.5150

distance-based algorithms that have a full topology knowledge. In Tab. I, the average iteration numbers, i.e., the average numbers of selected CR users, of the considered algorithms are reported. We note that our algorithm selects on average a number smaller than the numbers of the distance-based algorithms, thus allowing to save communication resources.

Fig. 10 shows P_d versus P_f for Top. 2, with the same simulation setting used for Fig. 9. Top. 2 is characterized by CR users more correlated than the CR users in Top. 1. This implies that the average numbers of CR users selected by the considered algorithms are smaller than the average numbers for Top. 1, as shown in Tab. I. Hence, the performances of all the algorithms are lower than those shown for Top. 1. Regarding the performance comparison, the proposed algorithm performs comparable with the distance-based algorithms, with a gain over Distance-Based-2. Moreover, our algorithm outperforms significantly the random selection. Fig. 9 and Fig. 10 show also P_d versus P_f when $Q = 200$ for Tops. 1 and 2, respectively. For both the topologies, the performances of the considered algorithms are lower than in the case where $Q = 500$, since T_s is decreased. In addition, the comparison among the algorithms results in the same conclusions as we detailed previously for $Q = 500$. Since, the average iteration numbers are comparable with those of Tab. I, they are not reported for brevity.

2) *Scenario B*: We analyze the effect of the threshold ϵ_d on the proposed selection, for $P_f = 10^{-2}$. ϵ_d ranges from 0.05 to e^{-1} .

In Fig. 11, the Average Maximum Correlation Coefficient (AMCC) among the CR users belonging to the selected set \mathcal{S} is reported versus ϵ_d for Top. 1. For the sake of comparison, we report also the AMCC of the other algorithms. Since the distance-based algorithms do not depend on ϵ_d , their values are constant. The results show that when ϵ_d increases, the AMCC

Fig. 11. Average Maximum Correlation Coefficient vs ϵ_d

among the selected CR users increases as well. The correlation increases almost linearly for the proposed algorithm, as a consequence of the *pruning* task implementation. Hence, ϵ_d controls the amount of correlation among the selected CR users, as expected. We note that our algorithm is able to assure for $\epsilon_d = e^{-1}$ the same AMCC of the distance-based algorithms that have a full topology knowledge.

Fig. 12 reports the average number of selected CR users versus ϵ_d , for Top. 1. The results show that ϵ_d controls also the cardinality of the selected set \mathcal{S} , since the threshold affects the extension of the research space. Similar considerations hold for Top. 2 and we do not report them for brevity. From the above considerations, it emerges that the ϵ_d value to be set is a trade-off between the amount of correlation tolerated by the application, and the number of collaborating CR users.

C. Performance Analysis with Correlated Multipath Fading

Two topologies, shown in Figs. 13 and 14, are considered. In both the topologies the number of CR users is $M = 36$ and the grid size is 10×10 m. The values of $\{g_i\}_{i=1}^M$ are randomly-generated according to a complex normal distribution with zero-mean and unitary variance. To model the spatial correlation, we adopt the proposed model (16), by

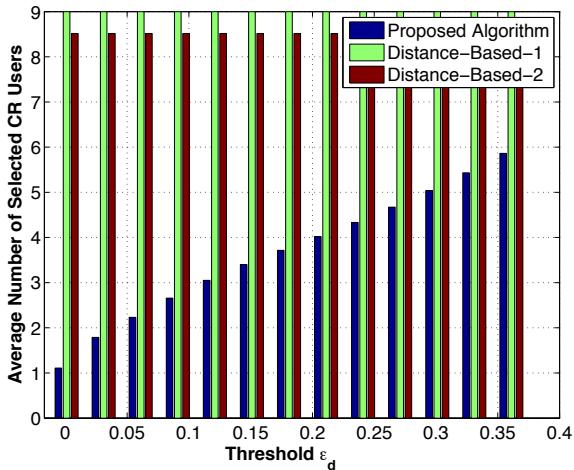
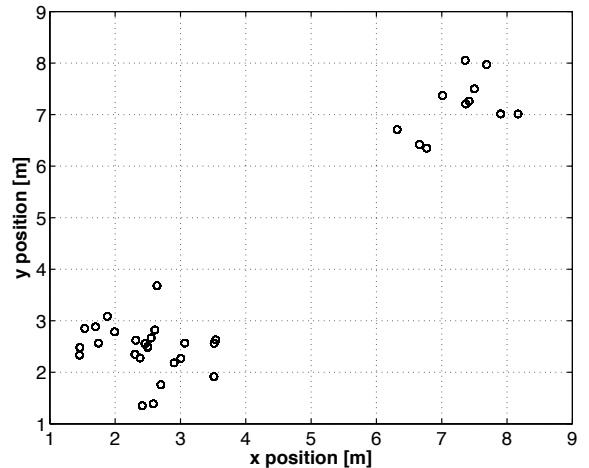
Fig. 12. Average Number of selected CR users vs ϵ_d 

Fig. 14. Top. 2 for Multipath

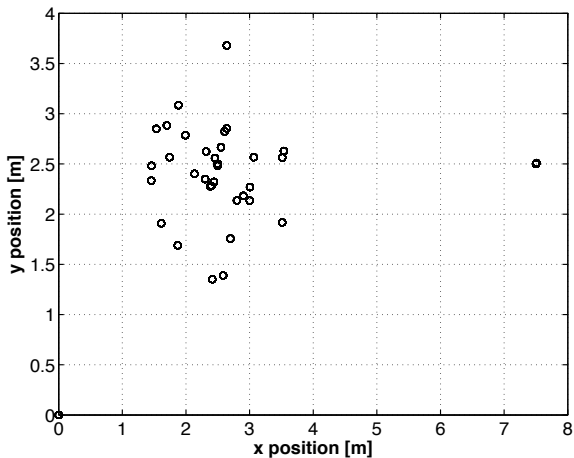
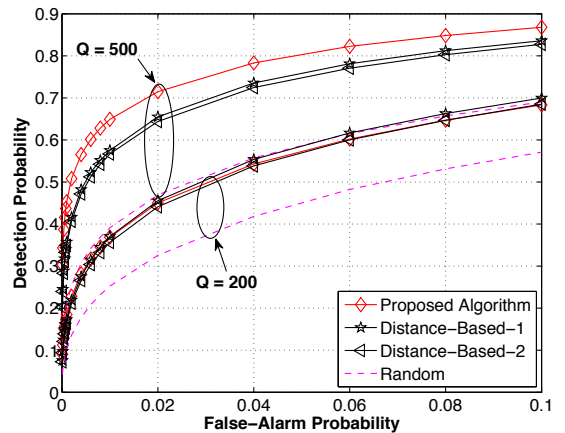


Fig. 13. Top. 1 for Multipath

Fig. 15. P_d vs P_f , Top. 1

assuming $f_c = 900$ MHz, $\zeta = 5$ and $\mu = \pi$. The results are obtained through 10^5 Monte Carlo runs. The arbitrary CR user in \mathcal{S} combines the sensing information by maximizing the deflection coefficient. In each run, the noise samples are independently generated according to a complex zero-mean normal distribution. ϵ_d is equal to 0.2 and the decorrelation distance for the distance-based algorithms is 1 m. P_f ranges from 10^{-4} to 10^{-1} .

1) *Scenario C*: We evaluate the performances of the algorithms when $SNR \triangleq \sigma_g^2/\sigma_n^2 = -12$ dB. σ_g^2 denotes the multipath channel variance and σ_n^2 the noise variance. Fig. 15 shows P_d versus P_f for Top. 1 and $Q = 500$. The proposed algorithm outperforms significantly the random selection, and it performs better than the two distance-based algorithms, although they have a full topology knowledge. The reason is that the knowledge of the mutual distances among the CR users is not sufficient to catch the correlation characteristics. In fact, the correlation due to the multipath does not depend only on the mutual distances (Section III). Instead, by estimating the correlation coefficients, the proposed algorithm accounts for the correlation channel conditions and therefore, it is more robust. This aspect is confirmed by the AMCC among the selected CR users. In fact, the maximum value for our

algorithm is $0.1633 < \epsilon_d$, significantly lower than the values of the other algorithms, equal to 0.4402, 0.3931 and 0.6782 for Distance-Based-1, Distance-Based-2 and the random algorithm, respectively. Tab. I reports the average iteration numbers of the algorithms, which shows that our algorithm selects a number of CR users smaller than the numbers of CR users selected in the distance-based algorithms.

Fig. 16 shows P_d versus P_f ($Q = 500$) for Top. 2, where the CR users are less correlated than in Top. 1. This implies that the average numbers of CR users selected by the considered algorithms are greater than the average numbers for Top. 1, as shown in Tab. I. Hence, the performances of the algorithms in terms of P_d are better than the performances associated with Top. 1. The proposed selection performs better than the two distance-based algorithms for the same reasons as for Fig. 15. Moreover, our algorithm outperforms significantly the random selection strategy. Fig. 15 and Fig. 16 show also P_d versus P_f when $Q = 200$ for Tops. 1 and 2, respectively. Our algorithm does not outperform the distance-based algorithms in Top. 1, since in presence of a strong correlation the correlation coefficient estimations, affected by the low Q -value, have a deep impact on the performance. Differently, the proposed algorithm outperforms all the algorithms in Top. 2, since in

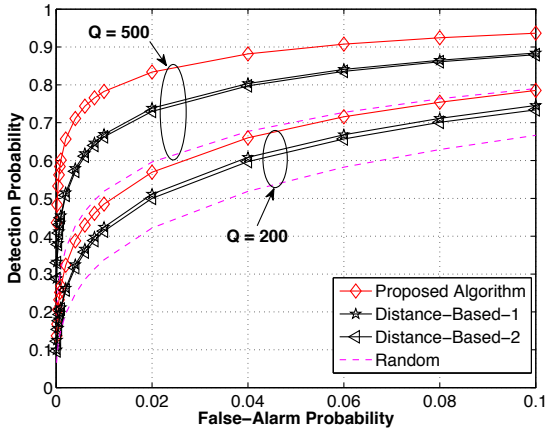


Fig. 16. P_d vs P_f , Top. 2

presence of a lower correlation the coefficient estimations have a lower impact on the performance.

VI. CONCLUSIONS

In this paper we developed a solution for the problem of uncorrelated user selection in mobile CR ad hoc networks, with the objective to increase the performance of cooperative spectrum sensing. We designed a fully distributed selection algorithm, which accounts for the changes in the network topology and in the channel conditions, by adaptively selecting uncorrelated CR users. The algorithm measures the correlation experienced by the CR users through the spatial correlation coefficient. To derive the correlation coefficient for multipath fading, we developed an analytical correlation model able to describe the correlation characteristics of mobile CR users. The proposed algorithm has been validated through simulations, and the results revealed the benefits of adopting the proposed correlation-aware selection for cooperative sensing.

ACKNOWLEDGEMENT

We thank B. Lo, Dr. Y. Tachwali, Dr. M. Caleffi, M. Pierobon and J. M. Jornet for their valuable feedbacks to improve this work.

APPENDIX A

PROOF OF PROPOSITION 1

We note that α_n^2 is the r.v. that describes the contribution of the n -th scatterer S_n to the total diffuse power P_r^{DIF} . For non-isotropic scattering, α_n^2 is a function, say $z(\cdot)$, of the AOA r.v. ϕ_{nl} , i.e., $\alpha_n^2 = \frac{P_r^{\text{DIF}}}{N} z(\phi_{nl})$. By substituting (11) in the definition of $R_{ik}^{\text{DIF}}(t, \tau)$, when N goes to infinite, we obtain:

$$R_{ik}^{\text{DIF}}(t, \tau) = P_r^{\text{DIF}} \int_{-\pi}^{\pi} e^{-j\frac{2\pi}{\lambda} [\xi_i(\phi) - \xi_k(\phi)]} e^{j2\pi f_{D_i} t \cos(\phi - \gamma_i)} e^{-j2\pi f_{D_k} (t - \tau) \cos(\phi - \gamma_k)} f(\phi) d\phi \quad (19)$$

In (19), $f(\phi)$ is the AOA-PDF, and $\xi_l(\phi)$ is the path length between the l -th CR user and the point on the ring of scatterers. If the radius R of the ring is greater than the CR distance, $R \gg d_{ik}$, the waves impinging the CR users are almost

parallel. Hence, by applying the law of cosines to the triangle R - CR_i - CR_k , and using $\sqrt{1+q} \simeq 1+q/2$, $\xi_l(\phi)$ is given by: $\xi_i(\phi) \simeq R + \frac{d_{ik}}{2} \cos(\theta_{ik} - \phi)$, $\xi_k(\phi) \simeq R - \frac{d_{ik}}{2} \cos(\theta_{ik} - \phi)$. By substituting $\xi_i(\phi)$ and $\xi_k(\phi)$ in (19), we obtain:

$$R_{ik}^{\text{DIF}}(t, \tau) = P_r^{\text{DIF}} \int_{-\pi}^{\pi} e^{-j\frac{2\pi}{\lambda} d_{ik} \cos(\theta_{ik} - \phi)} e^{j2\pi f_{D_i} t \cos(\phi - \gamma_i)} e^{-j2\pi f_{D_k} (t - \tau) \cos(\phi - \gamma_k)} f(\phi) d\phi \quad (20)$$

(20) holds for any PDF $f(\phi)$. By using in (20) the von Mises PDF, after some algebraic manipulation, (13) is obtained.

APPENDIX B

PROOF OF PROPOSITION 2

By substituting (10) in the definition of $R_{ik}^{\text{LOS}}(t, \tau)$, we have:

$$R_{ik}^{\text{LOS}}(t, \tau) = |g_{i,\text{LOS}}(t)| |g_{k,\text{LOS}}(t - \tau)| e^{-j2\pi \frac{(\xi_{P_i} - \xi_{P_k})}{\lambda}} e^{j2\pi [f_{D_i} t \cos(\phi_{P_i} - \gamma_i) - f_{D_k} (t - \tau) \cos(\phi_{P_k} - \gamma_k)]} \quad (21)$$

If $\xi_{P_i} \gg d_{ik}$ and $\xi_{P_k} \gg d_{ik}$, $\phi_{P_k} \simeq \phi_{P_i} \simeq \pi$. For this, by using $\sqrt{1+q} \simeq 1+q/2$ and by applying the law cosines to the triangle P - CR_i - CR_k , ξ_{P_i} is given by $\xi_{P_i} \simeq \xi_{P_k} - d_{ik} \cos(\theta_{ik})$. By substituting ξ_{P_i} in (21), (14) is obtained.

REFERENCES

- [1] J. M. III and J. G.Q. Maguire, "Cognitive radio: making software radios more personal," *IEEE Pers. Commun.*, vol. 6, no. 4, Aug. 1999.
- [2] I. F. Akyildiz, B. F. Lo, and R. Balakrishnan, "Cooperative spectrum sensing in cognitive radio networks: A survey," *Physical Communication (Elsevier) Journal*, vol. 4, no. 1, Mar. 2011.
- [3] A. Ghasemi and E. Sousa, "Collaborative spectrum sensing for opportunistic access in fading environments," in *Proc. IEEE DySPAN*, Nov. 2005.
- [4] J. Ma, G. Zhao, and Y. Li, "Soft combination and detection for cooperative spectrum sensing in cognitive radio networks," *IEEE Trans. Wireless Commun.*, vol. 7, no. 11, Nov. 2008.
- [5] W. Zhang and K. Letaief, "Cooperative spectrum sensing with transmit and relay diversity in cognitive radio networks," *IEEE Trans. Wireless Commun.*, vol. 7, no. 12, Dec. 2008.
- [6] K. Ben Letaief and W. Zhang, "Cooperative communications for cognitive radio networks," *Proc. IEEE*, vol. 97, no. 5, May 2009.
- [7] S. Mishra, A. Sahai, and R. Brodersen, "Cooperative sensing among cognitive radios," in *Proc. IEEE ICC*, vol. 4, Jun. 2006.
- [8] I. F. Akyildiz, W.-Y. Lee, and K. R. Chowdhury, "Crahs: Cognitive radio ad hoc networks," *Ad Hoc Networks*, vol. 7, no. 5, 2009.
- [9] Y. Selen, H. Tullberg, and J. Kronander, "Sensor selection for cooperative spectrum sensing," in *Proc. IEEE DySPAN*, Oct. 2008.
- [10] A. Malady and C. da Silva, "Clustering methods for distributed spectrum sensing in cognitive radio systems," in *Proc. IEEE MILCOM*, Nov. 2008.
- [11] M. Gudmundson, "Correlation model for shadow fading in mobile radio systems," *Electronics Letters*, vol. 27, no. 23, Nov. 1991.
- [12] P. Bello, "Characterization of randomly time-variant linear channels," *IEEE Trans. Commun. Syst.*, vol. 11, no. 4, Dec. 1963.
- [13] A. Abdi and M. Kaveh, "A space-time correlation model for multielement antenna systems in mobile fading channels," *IEEE J. Sel. Areas Commun.*, vol. 20, no. 3, Apr. 2002.
- [14] Z. Quan, S. Cui, and A. H. Sayed, "Optimal linear cooperation for spectrum sensing in cognitive radio networks," *IEEE J. Sel. Topics Signal Process.*, vol. 2, no. 1, Feb. 2008.
- [15] J. Man and Y. Li, "Soft combination and detection for cooperative spectrum sensing in cognitive radio networks," in *Proc. IEEE GLOBECOM*, Nov. 2007.
- [16] A. Goldsmith, *Wireless Communications*. Cambridge: Cambridge University Press, 2005.
- [17] A. Papoulis, *Probability, Random Variables, and Stochastic Processes*. New York: McGraw-Hill, 1984.
- [18] J. Fuhl, J.-P. Rossi, and E. Bonek, "High-resolution 3-d direction-of-arrival determination for urban mobile radio," *IEEE Trans. Antennas Propag.*, vol. 45, no. 4, Apr. 1997.

- [19] A. Abdi, J. Barger, and M. Kaveh, "A parametric model for the distribution of the angle of arrival and the associated correlation function and power spectrum at the mobile station," *IEEE Trans. Veh. Technol.*, vol. 51, no. 3, May 2002.
- [20] Y.-C. Liang, Y. Zeng, E. C. Peh, and A. T. Hoang, "Sensing-throughput tradeoff for cognitive radio networks," *IEEE Trans. Wireless Commun.*, vol. 7, no. 4, Apr. 2008.



Angela Sara Cacciapuoti received the Dr. Eng. degree summa cum laude in Telecom. Engineering in 2005, and the Ph.D degree with score excellent in Electronic and Telecom. Engineering in 2009, both from University of Naples Federico II. Since 2008, she is with the Dept. of Biomedical, Electronic and Telecom. Engineering (DIBET), University of Naples Federico II, as postdoctoral research fellow. From 2010 to 2011, she has been with Broadband Wireless Networking Laboratory, Georgia Institute of Technology, as visiting researcher. In 2011, she

has also been with NaNoNetworking Center in Catalunya (N3Cat), Universitat Politècnica de Catalunya (UPC), as visiting research. Her current research interests are in cognitive radio networks and non-stationary signal processing.



Ian F. Akyildiz received the B.S., M.S., and Ph.D. degrees in Computer Engineering from the University of Erlangen-Nürnberg, Germany, in 1978, 1981 and 1984, respectively. Currently, he is the Ken Byers Chair Professor with the School of Electrical and Computer Engineering, Georgia Institute of Technology, Atlanta, the Director of Broadband Wireless Networking Laboratory and Chair of the Telecommunication Group at Georgia Tech. In June 2008, Dr. Akyildiz became an honorary professor with the School of Electrical Engineering at Universitat

Politécnica de Catalunya (UPC) in Barcelona, Spain. He is also the Director of the newly founded N3Cat (NaNoNetworking Center in Catalunya). He is also an Honorary Professor with University of Pretoria, South Africa, since March 2009. He is the Editor-in-Chief of Computer Networks (Elsevier) Journal, and the founding Editor-in-Chief of the Ad Hoc Networks (Elsevier) Journal, the Physical Communication (Elsevier) Journal and the Nano Communication Networks (Elsevier) Journal. Dr. Akyildiz serves on the advisory boards of several research centers, journals, conferences and publication companies. He is an IEEE FELLOW (1996) and an ACM FELLOW (1997). He received numerous awards from IEEE and ACM. His research interests are in nano-networks, cognitive radio networks and wireless sensor networks.



Luigi Paura received the Dr. Eng. degree summa cum laude in Electronic Engineering in 1974 from University of Napoli Federico II. From 1979 to 1984, he was with the Dept. of Biomedical, Electronic and Telecom. Engineering, University of Naples Federico II, first as an Assistant Professor and then as an Associate Professor. Since 1994, he has been a Full Professor of Telecom.: first, with the Dept. of Mathematics, University of Lecce, Italy; then, with the Dept. of Information Engineering, Second University of Naples; and, finally, from

1998 he has been with the Dept. of Biomedical, Electronic and Telecom. Engineering, University of Naples Federico II. He also held teaching positions at University of Salerno, at University of Sannio, and at University Parthenope of Naples. In 1985-86 and 1991 he was a visiting researcher at Signal and Image Processing Lab, University of California, Davis. His research interests are mainly in digital communication systems and cognitive radio networks.